



# VIPERLAB

FULLY CONNECTED VIRTUAL AND PHYSICAL  
PEROVSKITE PHOTOVOLTAICS LAB

**D 8.7**

**Identification of optical markers to control  
the timing for quenching of  
Perovskite PV layers**

**DELIVERABLE  
REPORT**

Version: 1.2

Date: 30.11.2023



FULLY CONNECTED VIRTUAL AND  
PHYSICAL PEROVSKITE PHOTOVOLTAICS LAB  
VIPERLAB

### DELIVERABLE

D 8.7 IDENTIFICATION OF OPTICAL MARKERS TO CONTROL THE TIMING FOR QUENCHING  
OF PEROVSKITE PV LAYERS

#### Project References

Project Acronym	VIPERLAB
Project Title	Fully connected <b>virtual</b> and physical <b>perovskite</b> photovoltaics <b>lab</b>
Project Coordinator	Helmholtz-Zentrum Berlin
Project Start and Duration	1st June 2021, 42 months

#### Deliverable References

Deliverable No	D 8.7
Type	Report
Dissemination level	Public
Work Package	WP8
Lead beneficiary	HI ERN FZJ
Due date of deliverable	30 November 2023
Actual submission date	30 November 2023

#### Document history

Version	Status	Date	Beneficiary	Author
1.0	First Draft	28-11-2023	FZJ	M. Sytnyk
1.1	Updated Draft	29-11-2023	FZJ	M. Sytnyk
1.2	Reviewed Draft	30-11-2023	TNO	S.C.Veenstra

## DISCLAIMER

'Fully connected virtual and physical perovskite photovoltaics lab' VIPERLAB is a Collaborative Project funded by the European Commission under Horizon 2020. Contract: 101006715, Start date of Contract: 01/06/2021; Duration: 42 months.

The authors are solely responsible for this information, and it does not represent the opinion of the European Community. The European Community is not responsible for any use that might be made of the data appearing therein.



## TABLE OF CONTENT

<b>LIST OF ABBREVIATIONS .....</b>	<b>4</b>
<b>EXECUTIVE SUMMARY .....</b>	<b>5</b>
<b>1. INTRODUCTION TO IN-SITU CHARACTERIZATION IN PEROVSKITE SOLAR CELLS .....</b>	<b>5</b>
1.1 X-RAY SPECTROSCOPY.....	6
1.2 UV-VIS AND PL SPECTROSCOPIES.....	6
1.3 IMPORTANCE OF OPTICAL MARKERS IN CONTROLLING PEROVSKITE LAYERS.....	9
<b>2. METHODS.....</b>	<b>10</b>
2.1 DESCRIPTION OF THE PROCESS AND TECHNIQUES.....	10
2.2 ANALYSIS AND ORGANIZATION OF OPTICAL MARKER DATA.....	14
<b>3. SELECTION OF OPTICAL MARKERS .....</b>	<b>15</b>
<b>4. THE ROLE OF PL MARKERS IN CONTROLLING THE TIMING FOR QUENCHING</b>	<b>18</b>
<b>5. CASE STUDY: PEROVSKITE SOLAR CELL FABRICATION .....</b>	<b>21</b>
<b>6. CONCLUSION.....</b>	<b>24</b>
<b>7. REFERENCES .....</b>	<b>26</b>



## LIST OF ABBREVIATIONS

**ATM.:** Operational Atmosphere

**CB:** Chlorobenzene

**CV:** Coefficient of Variation

**FF:** photovoltaic Fill Factor

**FWHM:** Full Width at Half Maximum

**GIWAX:** Grazing-Incidence Wide-Angle X-ray Scattering

**IV:** Current-Voltage

**Jsc:** Short-Circuit Current

**HT:** High-Throughput

**LED:** Light-Emitting Diode

**MPPT:** Maximum Power Point Tracking

**PCE:** Power Conversion Efficiency

**PL:** Photoluminescence Spectroscopies

**PSK:** Perovskite

**PSCs:** Perovskite Solar Cells

**PV:** Photovoltaics

**RH:** Relative Humidity

**TRPL:** Time-Resolved Photoluminescence

**VAG:** Vacuum-Assisted Growth

**Voc:** Open-Circuit Voltage

**XRD:** X-Ray Diffraction

**UV-Vis:** UV-Visible Spectroscopy

**WL:** Wavelength



## EXECUTIVE SUMMARY

This report dives into the realm of in-situ characterization in perovskite solar cells, unraveling key insights through various optical markers. Expanding on the significance of UV-Vis and photoluminescence (PL) spectroscopies, it explores their role in controlling perovskite layers, with a focus on quenching timing. The employed multi-faceted approach, integrated with the SPINBOT automated platform, uncovered crucial findings. UV-Vis absorption spectra exhibited uniformity, signaling consistent film thickness, yet additional markers were needed for comprehensive quality assessment. PL spectroscopy emerged as a robust metric, revealing insights into film microstructure and radiative recombination efficiency. This knowledge played a pivotal role in guiding the timing of quenching during film fabrication. Spatial PL intensity distribution maps showcased variations based on antisolvent quenching timing, underscoring PL intensity as a key indicator of film homogeneity. Applying these insights to perovskite solar cell fabrication, the report assessed device performance metrics, such as photocurrent density, open-circuit voltage, fill factor, and power conversion efficiency. Correlating PL findings with electrical characteristics validated the role of PL markers in optimizing device performance. In essence, this study establishes the critical importance of selecting appropriate optical markers to control quenching timing in perovskite PV layers. This strategic selection is instrumental in ensuring uniform film quality and enhancing the overall performance of perovskite solar cells, contributing significantly to advancements in photovoltaic technology.

## 1. INTRODUCTION TO IN-SITU CHARACTERIZATION IN PEROVSKITE SOLAR CELLS

Perovskite solar cells have emerged as a prominent technology in photovoltaics, owing to their remarkable properties such as high absorption coefficient, tunable bandgap, and cost-effective production methods. These solar cells comprise a perovskite-structured compound, typically a hybrid organic-inorganic lead and/or tin halide-based material, which acts as the light-harvesting active layer. The performance and stability of these solar cells are heavily influenced by the quality of the perovskite layers, making their precise control during fabrication crucial.

In this context, in-situ and “online” characterization techniques are pivotal. They provide real-time monitoring of the perovskite layer formation and allow immediate adjustments during fabrication. This real-time monitoring is vital for understanding the dynamics of film formation and crystallization, which are crucial to achieving optimal device performance and reproducibility.

In-situ characterization techniques, particularly those based on spectroscopical methods like X-ray diffraction (XRD), UV-visible (UV-Vis), and Photoluminescence (PL) spectroscopies, have become indispensable in this context. These techniques allow real-time monitoring and optimization of the perovskite layer formation, which is crucial for achieving high-performance solar cells.



## 1.1 X-ray spectroscopy

Building upon the foundational understanding of perovskite solar cells, the Gratia et al. study [1] serves as a critical advancement in the field, especially through the application of in-situ X-ray diffraction. This technique has unveiled key aspects of crystallization in mixed ion perovskites, integral to developing these solar cells. Specifically, the study reveals the presence of 3D hexagonal polytypes, namely 6H and 4H, in  $(\text{FAPbI}_3)_x(\text{MAPbBr}_3)_{1-x}$ . These in situ XRD measurements are instrumental in providing a comprehensive understanding of the phase transformations that occur during annealing and how varying concentrations of Cs and Br influence the crystallization process. The study notes a distinct sequence in the crystallization process, transitioning from 2H to 4H, then to 6H, and finally to 3R(3C), a pattern like that observed in transition metal oxide perovskites under extreme conditions. A notable finding from this research is that introducing more than 3%  $\text{Cs}^+$  cations into the lattice effectively inhibits the formation of these hexagonal polytypes, which has significant implications for enhancing the stability and reproducibility of the devices.

Further expanding on the theme of crystallization and its impact on perovskite solar cells (PSCs), the 2021 review by Qin et al. [2] systematically explores the intricate relationships between the crystallization process, optical markers, and the performance of PSCs by in situ GIWAXS. This comprehensive study underscores the vital importance of controlled crystallization rates and film uniformity in the production of defect-minimized films, which directly affect the performance of PSCs. The research highlights the necessity of maintaining a single, stable perovskite phase to minimize charge trap sites, thereby enhancing the efficiency and longevity of the solar cells. Additionally, Qin et al. draw attention to the link between the films' morphology and grain size and the solar cells' efficiency, noting that larger grains and smoother morphologies contribute to reduced charge recombination and improved charge transport. Furthermore, the review delves into the direct impact of optical properties such as absorption and PL on the quality of the perovskite layer. It emphasizes that high absorption efficiency across the relevant solar spectrum and strong, stable photoluminescence indicate low non-radiative recombination, which is crucial for achieving high-efficiency PSCs. The study also examines the influence of additives and specific processing conditions on modulating the crystallization process, demonstrating their role in improving film quality and crystal orientation, thereby enhancing phase purity.

## 1.2 UV-Vis and PL Spectroscopies

UV-Vis spectroscopy has played an even more significant role in advancing perovskite solar cells. A study [3] delved into the key optical features of perovskite films, including UV-Vis reflectance and PL. These features are essential for monitoring various aspects of the film's formation. UV-Vis reflectance is particularly useful for observing the thinning behavior of wet films during spin-coating, providing critical insights into the film's thickness and uniformity. These aspects are vital for achieving a homogenous film, a crucial factor for high-quality solar cell layers.

Additionally, the study highlights the role of PL tracking, conducted during both spin-coating and annealing stages. Strong and narrow PL peaks indicate a high-quality perovskite phase, essential for efficient solar cell operation. The study also explores how various fabrication parameters, such as precursor concentration, spin-coating parameters, annealing conditions, and the use of anti-



solvents, influence these optical characteristics. It was observed that higher precursor concentrations can delay the onset of crystallization, thereby impacting the dynamics of film formation. Spin-coating parameters, including spin speed and duration, significantly affect the film's thinning behavior and, consequently, its uniformity. Annealing conditions are critical in determining the crystallization process, with optimal conditions necessary to achieve a high-quality crystalline structure. Applying anti-solvents during spin-coating is a key factor influencing crystallization kinetics and phase formation, observable through changes in PL characteristics.

Another study employing in-situ spectroscopy [4] during the spin coating and annealing stages of mixed bromide-iodide perovskite films revealed the critical influence of halide ratios in the precursor solution on the crystallization path and phase homogeneity. This research demonstrates that the ratio of bromide to iodide in the precursor solutions significantly dictates the phase formation pathway, thus influencing the ionic homogeneity, morphology, and optoelectronic properties of the resultant films. This approach not only sheds light on the complex formation processes of mixed halide perovskites but also underscores the importance of these processes in optimizing the efficiency and stability of perovskite solar cells.

Furthermore, the work of Christian Camus and his team [5] introduces high-speed spectral reflectance measurements for in-situ monitoring of perovskite layer formation. This method effectively captures the perovskite layer's dynamic evolution during the spin-coating and annealing stages. The evolution of reflectance spectra during these stages is particularly telling, with the transition from a  $\text{PbI}_2$  precursor to the final perovskite structure being clearly tracked. During spin-coating, distinct interference patterns and fringes appear, providing immediate feedback on the process. A notable shift in the absorption edge, from approximately 480 nm to around 440 nm, is observed during this stage, signaling compositional changes in the solution. This shift is crucial for differentiating between chemical changes and film thinning. During annealing, the method focuses on shifts in the absorption edge to detect phase transitions, offering more profound insights into film formation kinetics, composition, and identifying any potential phase segregations or inhomogeneities. By tracking these minute-by-minute spectral changes, this method aids in determining the optimal annealing time and conditions, which are essential for the consistent and reproducible formation of high-quality perovskite layers.

In the realm of perovskite solar cell research, a recent study [6] focused on the formation kinetics of bromide-based triple cation perovskite ( $\text{Cs}_{0.05}\text{MA}_{0.10}\text{FA}_{0.85}\text{PbBr}_3$ ) thin films, revealing the significant impact of precursor solution concentration during the spin-coating process. The study employed in-situ UV-vis and PL spectroscopy to investigate this phenomenon. It was found that lower solution concentrations led to expedited nucleation and growth kinetics, resulting in earlier crystallization and faster growth of crystallites. This finding is crucial as it indicates that adjusting the solution concentration can markedly influence the morphological and optoelectronic properties of the resulting films. Films produced from higher concentrated solutions exhibited more defined cubic grains but also displayed issues such as roughness and inhomogeneity in thickness. These insights highlight the importance of carefully controlling the solution concentration to balance film quality, encompassing attributes such as uniformity, smoothness, and optimized thickness. These factors are essential for developing high-efficiency and stable perovskite solar cells, underscoring the critical role of process parameters in influencing the formation and quality of perovskite films.





Another groundbreaking study by Fong et al. [7] achieved a significant milestone in fabricating high-efficiency perovskite solar cells, particularly under high-humidity conditions ( $55 \pm 5\%$  RH). This research utilized in situ time-resolved UV-vis spectrometry to provide an in-depth analysis of the drying kinetics and crystallization behavior of perovskite films during blade-coating. A key finding was the effective use of varying air-knife blowing velocities to control the film formation process precisely. This technique created solar cells with impressive power conversion efficiencies, reaching 21.1% for small-area and 18.0% for larger-area devices. The study emphasizes the critical role of in-situ UV-vis spectrometry in monitoring film formation in real time. By fine-tuning parameters such as air-knife blowing velocities, the researchers optimized the perovskite films' nucleation and growth processes, resulting in films with fewer non-radiative recombination centers and improved quality. The optical markers identified in the UV-Vis spectra, including a sharp, redshifted absorption edge and strong, narrow photoluminescence peaks, indicated the formation of high-quality perovskite phases. These optical signatures correlate with larger grain size, enhanced crystallinity, reduced defect density, and minimal non-radiative recombination losses, contributing significantly to the enhanced efficiency of the solar cells. Furthermore, the study observed uniform reflectance spectra during film formation, suggesting even film thickness and consistent crystallization, both of which are crucial for achieving optimal solar cell performance.

The subsequent important work of Fabian Schackmar and his team [8] introduces a novel approach to perovskite thin-film formation through Vacuum-Assisted Growth (VAG). This technique, incorporating inkjet printing and blade coating methods, emphasizes a vacuum-based drying phase to expedite solvent evaporation and concentrate precursor salts. This step is crucial as it sets the stage for subsequent nucleation and crystal growth, which commence once a critical level of supersaturation is achieved. The process concludes with the venting of the vacuum chamber and a final thermal annealing step, which is essential for refining the crystalline structure of the perovskite layer. Key to this study is the use of in-situ monitoring techniques, including PL spectroscopy and thermography, allowing for real-time observations of film changes. Parameters such as evacuation rate, ink composition, wet-film thickness, and substrate properties are fine-tuned for optimal film morphology and crystal quality, enhancing solar cell performance. This fine-tuning is aimed at optimizing the film's morphology and crystal quality, directly contributing to the enhanced performance of the solar cells. Notably, the study focuses on key optical features such as PL intensity and peak wavelength (WL), which offer valuable insights into the nucleation and crystal growth phases. Reflection transients observed during the VAG process provide additional information regarding changes in surface morphology and film thickness. The findings suggest that a faster drying rate, achieved through rapid evacuation, is integral to forming high-quality films, as slower rates could result in defects like pinholes and needle-like crystallites. The thickness of the wet film is shown to significantly impact nucleation onset and crystallization dynamics, with thicker films requiring prolonged evaporation, thus affecting the quality of the perovskite layer.

Moreover, changes in the PL peak WL during the drying phase indicate ion incorporation and the completeness of film formation. A stable and high PL intensity post-nucleation is a marker of efficient radiative recombination and good film quality. In contrast, consistent PL peak WL patterns during film formation are vital for ensuring uniformity and addressing potential composition issues. Lastly, observing a smooth and consistent reflection transient suggests a uniform film surface, which is crucial for the efficient performance of solar cells.



Complementing these findings, our recent study [9] introduces SPINBOT, an advanced automated platform designed for optimizing the fabrication of metal-halide perovskite films and solar cells. This platform stands out for its precise control over various processing parameters, achieving a significant milestone in the field of perovskite solar cell processing. Notably, SPINBOT has successfully produced perovskite solar cells at ambient conditions with a remarkable 21% power conversion efficiency and enhanced photo-thermal stability. This achievement is attributed to optimizing parameters such as anti-solvent quenching conditions and atmospheric settings. A critical finding from this study is the importance of high PL intensity and PL surface homogeneity across the entire substrate, which are critical factors in fabricating efficient solar cells. The study's significance lies in demonstrating reasonable process control and reproducibility, as evidenced by the minimal coefficient variance in photoluminescence intensity. It underscores the platform's capability to produce high-quality perovskite solar cells consistently.

### 1.3 Importance of Optical Markers in Controlling Perovskite Layers

Based on the extensive literature on perovskite solar cells, it becomes evident that the quality of the perovskite layers deeply influences the performance and stability of these cells. Studies have consistently shown that in-situ and online characterization techniques, particularly spectroscopic methods such as XRD, UV-Vis, and PL spectroscopies, are crucial for real-time monitoring and optimization of the perovskite layer formation. These methods have been instrumental in understanding the dynamics of film formation and crystallization, thereby enabling optimal device performance and reproducibility. For instance, the Gratia et al. study [1] used in situ XRD to uncover key aspects of crystallization in mixed ion perovskites, crucial for solar cell development. Similarly, the review by Qin et al. [2] highlighted the importance of controlled crystallization rates, film uniformity, and the impact of optical properties such as absorption and photoluminescence on the perovskite layer's quality. These studies underscore the significance of maintaining a stable perovskite phase and optimizing film morphology and grain size for enhanced solar cell efficiency.

Further, studies [3-7] have delved deep into UV-Vis and PL spectroscopies, emphasizing their role in monitoring film formation, and influencing crystallization kinetics and phase formation. These studies have provided insights into how various fabrication parameters affect the optical characteristics of the perovskite films, thus influencing the overall efficiency and stability of the solar cells.

Notably, post-process measurement markers have been highlighted in these studies, suggesting that the main correlations between measurement markers and solar cell performance come primarily from data acquired after fabrication. This emphasizes that layers' post-process analysis is crucial in understanding solar cells' ultimate efficiency and stability.

In alignment with the critical role of in-situ characterization and post-process measurement of optical markers in perovskite solar cells, our recent investigation [9] further advances this field by enhancing the high-dimensional processing parameter space for perovskite thin-film fabrication. Utilizing the state-of-the-art SPINBOT platform, our study successfully optimized several key aspects of the fabrication process. We established a significant correlation between film uniformity, the timing of antisolvent quenching, and the reliance on Photoluminescence measurements as reliable device



performance indicators. Our approach enabled us to fabricate perovskite solar cells that adapted to ambient conditions and achieved 21% power conversion efficiency. This optimization was closely tied to continuously monitoring optical markers throughout the fabrication step of anti-solvent quenching. By leveraging these optical markers, we were able to refine the quality of the perovskite layers significantly, ultimately leading to enhanced performance and efficiency of the solar cells.

## 2. METHODS

Before discussing the specific methods used, it is essential to introduce the SPINBOT platform, a key element of our experimental design. This tailor-made robotic system enables precise manipulation and processing of perovskite films, which is crucial for our research. Using the SPINBOT, we aim to identify optical markers that can reliably indicate the correct processing conditions for perovskite PV layers. To achieve this, we employed various optical characterization methods, such as steady-state and time-resolved PL, along with UV-Vis absorption. A critical aspect of our method involves the careful timing of chlorobenzene anti-solvent quenching. This process demands exact control over the speed at which the anti-solvent is ejected and the timing between the spin casting of the perovskite layer and the quenching step. The accuracy of these timings is essential for ensuring the uniformity and quality of the perovskite films. Our optimization efforts are focused on fine-tuning the anti-solvent quenching process to improve the performance metrics of the solar cells, such as the current-voltage (IV) characteristics, fill factor (FF), power conversion efficiency (PCE), and maximum power point tracking (MPPT) stability.

### 2.1 Description of the Process and Techniques

The SPINBOT platform, a homemade robotic system, was central to our experimental methodology. This platform, illustrated in Figure 1, incorporates an exact robot arm capable of movement along four axes: X, Y, Z, and R. The arm functionalities are complemented by a liquid handling pipette for meticulous solution management, a substrate handling gripper for sample handling, and mini spin coaters to ensure uniform thin-film processing. Using pipette tips and 96-well microplates facilitates stocking solutions and anti-solvents, providing a high degree of experimental versatility (Figure 1A) [9].

High-throughput (HT) characterization techniques were employed to analyze samples fabricated via the SPINBOT platform. This process integrated steady-state PL, UV-Vis absorption, and time-resolved PL spectroscopies to monitor the optoelectronic properties of the perovskite films comprehensively. This high-throughput approach enabled the simultaneous analysis of multiple samples, enhancing the efficiency and depth of our experimental investigations (Figure 1B).

The data collected from the SPINBOT platform was analyzed and organized through a step-by-step optimization workflow depicted in Figure 1C. This workflow consisted of five steps designed to fine-tune a specific aspect of the perovskite film formation process by exploring 61 experimental parameter combinations.

In Step 1, operational atmospheres (ATM.) were manipulated inside the spin-coater chamber to identify the optimal conditions for film deposition. This involved testing various atmospheric



conditions, including the presence or absence of inert gases like nitrogen and vacuum suction levels, to determine their effects on the film's crystallization and morphology.

Step 2 focused on optimizing the tip height during the chlorobenzene (CB) anti-solvent quenching process. Precise adjustment of the dispensing tip height is essential to control the film's surface interaction with the anti-solvent, thereby affecting the film's uniformity and crystallinity.

The dispense velocity of CB is the focus of Step 3. By varying the ejection speed of the anti-solvent, we could influence the rate of film formation and the kinetic pathway of crystal growth, which are crucial for achieving a high-quality perovskite layer.

Step 4 adjusted the rotation speed during the high-speed stage of spin coating. The spin rate directly impacts the thinning behavior of the wet films and, consequently, the uniformity and thickness of the resulting perovskite layers.

Lastly, Step 5 combines the CB volume with the dispense timing delay. This step is crucial for determining the precise moment and quantity of anti-solvent introduction, which could significantly alter the nucleation and growth of the perovskite crystals.

The methodical application of these optimization steps is crucial in refining our understanding of the perovskite film formation process, focusing on identifying the optical markers critical for the quality control of perovskite PV layers.

Building on the SPINBOT platform capabilities, we further refined the perovskite film deposition technique through the quasi-static on-the-fly spin-coating mode, as represented in Figure 2 [9]. This method addresses the challenge of achieving uniform precursor distribution and film thickness. Figure 2A illustrates the precise control achieved over the deposition process. In the initial stage, the substrate rotates slowly, allowing the precursor to be evenly dispensed while the pipette tip moves from the center to the substrate edge. This gradual movement ensures that the entire substrate surface interacts with the precursor solution, laying the groundwork for a uniformly coated film. Once the solution is dispensed, the spin coater accelerates to the target speed, effectively spreading the solution and facilitating solvent evaporation. The simulation pattern depicted in Figure 2B visualizes the trajectory of the solution during the on-the-fly spin-coating process. The concentric distribution pattern ensures an even coating.



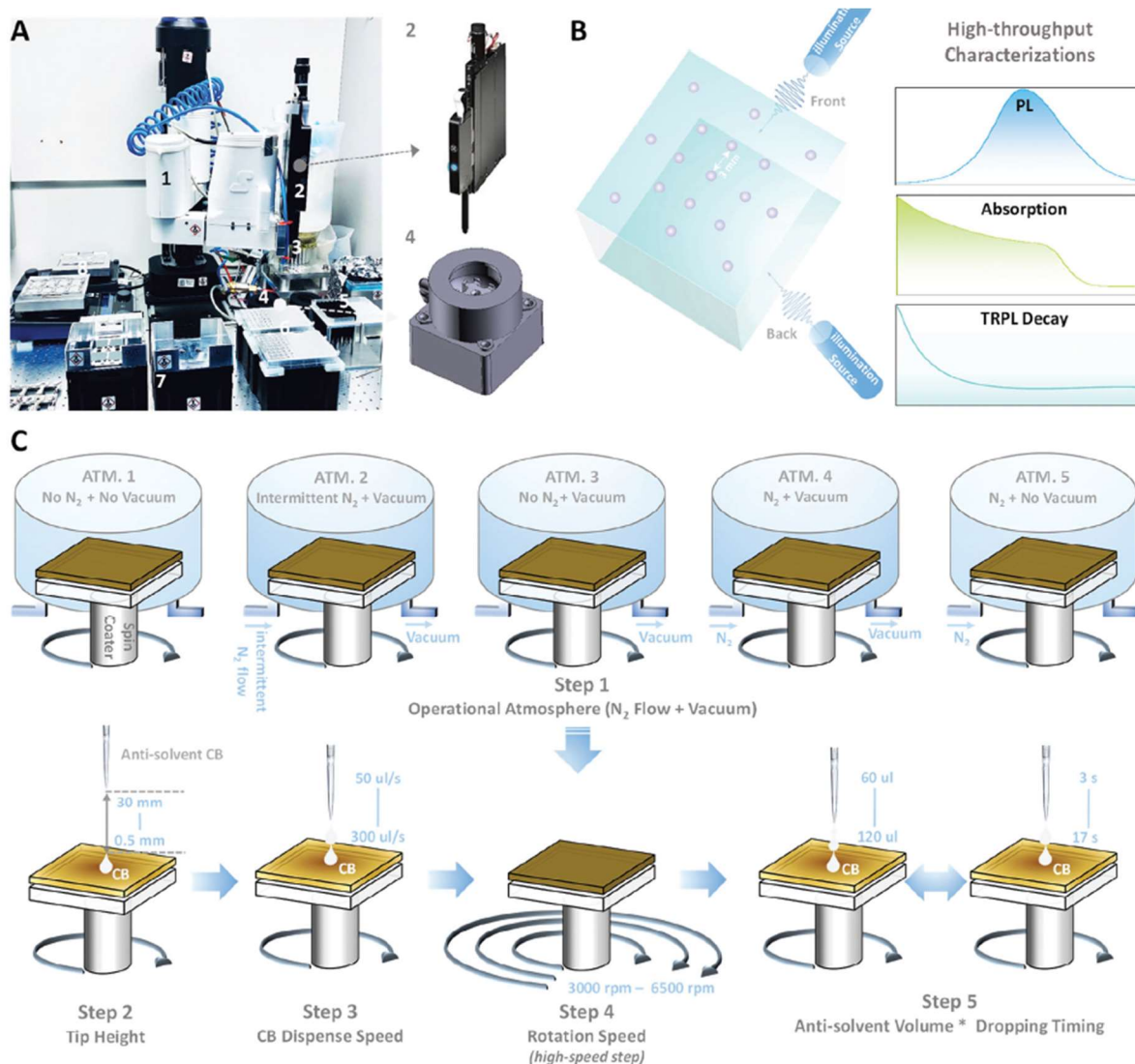


Figure 1: Overview of the SPINBOT platform and optimization workflow. A) The SPINBOT platform, illustrated with a robot arm (1) capable of precise four-axis movements: X, Y, Z, and R-axis, for versatile handling and positioning. The system includes a liquid handling pipette (2) for accurate fluid dispensation, a substrate handling gripper (3) for secure sample manipulation, mini spin coaters (4) for uniform film application, and pipette tips (5) for precision dispensing. Additionally, 96-well microplates (6) serve as reservoirs for solutions and anti-solvents, while carrier holders (7) and hotplates (8) facilitate the preparation and processing of samples. B) A schematic representation of the high-throughput characterization methods applied to samples processed by the SPINBOT platform, showcasing the steady-state PL, UV-Vis absorption, and time-resolved PL spectroscopies, providing a triad of analytical techniques for in-depth material characterization. C) An illustrative sequence of the optimization workflow with five critical steps, each exploring a unique set of 61 experimental parameter combinations. The schematic details the optimization of ATM. within the spin-coater chamber (Step 1), adjustment of tip height during CB quenching (Step 2), calibration of CB dispense velocity (Step 3), tuning of rotation speed for spin-coating (Step 4), and the combination of CB volume and delayed dispensing time (Step 5) [9].



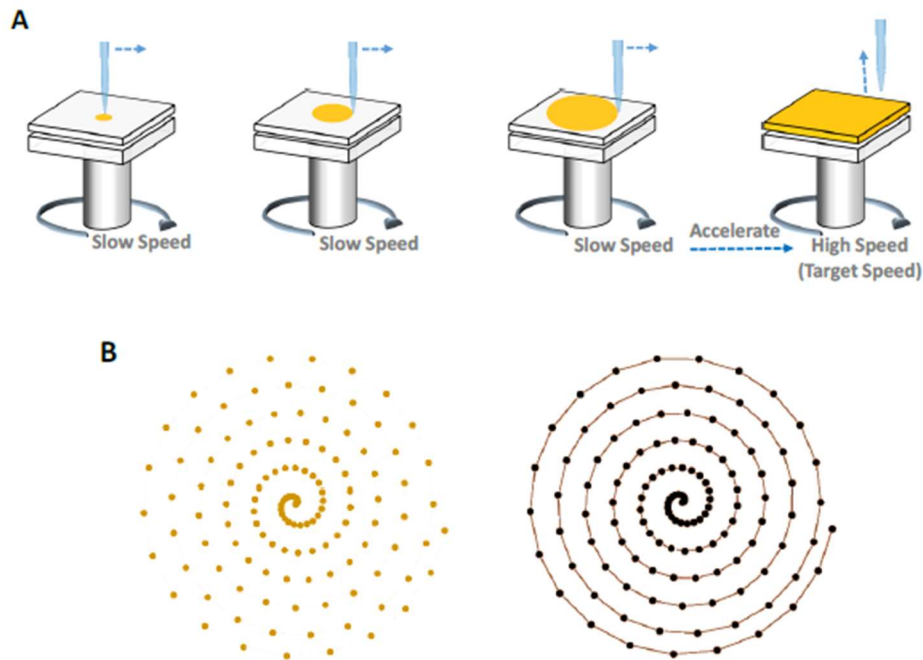


Figure 2: Quasi-static on-the-fly spin-coating for PSK films. A) Depiction of the controlled precursor dispensing on a slowly rotating substrate, ensuring uniform distribution across the surface for consistent film thickness. B) Simulation pattern representing the even spread of the solution, crucial for achieving homogenous films with uniform optical markers, as part of the SPINBOT platform advanced coating technique [9].

Expanding on the methodologies outlined in Figure 3 provides visual support for the tools utilized in preparing and analyzing perovskite films. Panel A shows a 96-well polypropylene microplate, which serves as a reservoir for perovskite precursor solutions. Such a microplate is integral to the SPINBOT system, ensuring a consistent and reproducible supply of precursor material for the spin-coating process.

Panel B of Figure 3 presents a carrier substrate with eight distinct samples, all fabricated by the SPINBOT in ambient air conditions. The ability to process multiple samples simultaneously under ambient conditions not only streamlines the experimental workflow but also reflects the real-world applicability of the methodology. The photographs in Figure 3 compare the films under different lighting, showing how the films look in natural light and when backlit by an LED panel. This helps us briefly check the films clarity and color uniformity, which are primary indicators of their overall quality. These visual checks are a quick way to spot any obvious issues with the films before we move on to more detailed tests like photoluminescence and absorption that give us a deeper understanding of the films' properties.

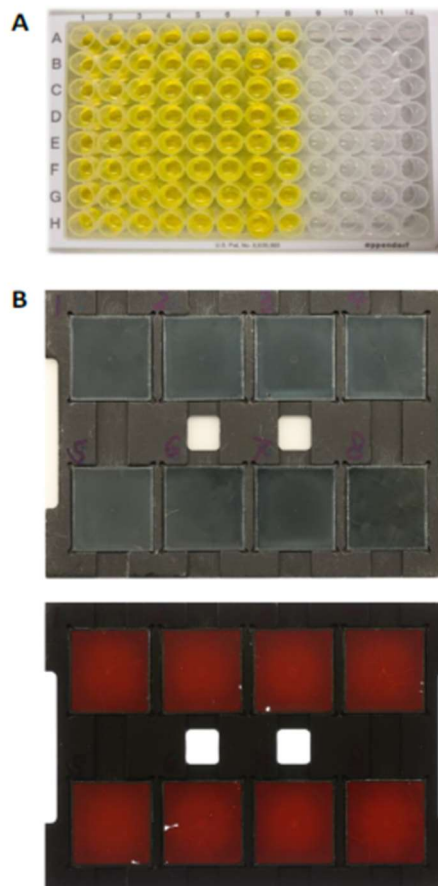


Figure 3: Visual documentation of PSK films preparation and visual quality assessment. A) Image of a 96-well polypropylene microplate for sourcing perovskite precursor solutions in the SPINBOT platform. B) Top: Carrier substrate displaying eight perovskite film samples processed by SPINBOT under ambient conditions. Bottom: The same samples are illuminated with an LED backlight to evaluate transparency and color uniformity, providing a preliminary visual quality check [9].

## 2.2 Analysis and Organization of Optical Marker Data

In our research to identify and define optical markers for controlling quenching timing in perovskite PV layers, we applied statistical analysis to ensure the precision and consistency of our findings. This involved examining a wide array of optical spectroscopy data, encompassing many samples. Our primary focus is analyzing variations in peak positions, widths, and integrals from absorption and PL spectra and differences in time decay for TRPL, aiming to pinpoint indicators of film quality and potential irregularities.

Utilizing the SPINBOT platform, we embarked on a methodical sequential optimization process. This process entailed adjusting critical variables like the height at which the anti-solvent is dispensed and the velocity of its application. These parameters were explicitly chosen for their potential to impact the optical characteristics of the films, which are central to identifying reliable optical markers. For



instance, changes in the dispensing aspects of chlorobenzene were observed to cause significant shifts in the PL spectra. These shifts are crucial, as they directly correlate with the crystal homogeneity and quality of the films, aligning with our goal to refine the timing of quenching in the PV layer fabrication.

To facilitate a clear visualization of these effects, we also employed colour maps to illustrate the variations in the optical properties across the films. These representations provided an intuitive understanding of how each alteration in the processing parameters influenced film uniformity and quality.

In the final stage of our development, our optimization efforts concentrated on refining the anti-solvent quenching process to evaluate the performance metrics of the solar cells. This refinement is crucial for improving key aspects such as IV characteristics, FF, PCE, and MPPT stability. We could influence these performance metrics by precisely adjusting the quenching process parameters.

### 3. SELECTION OF OPTICAL MARKERS

Building upon the robust methodology established in the SPINBOT platform and the selected characterization techniques described earlier, we first focus on the main stage of selecting optical markers. The initial step in our analysis method involves the aggregation of optical spectra from many test points across each sample within 8 sample batches per each testing step. This aggregation is critical to capture the perovskite films' optical properties completely. As mentioned above, our spectroscopy selection includes UV-Vis absorbance, photoluminescence, and TRPL, which provide a multi-faceted view of the films' optoelectronic characteristics.

Turning to UV-Vis absorption spectroscopy, Figure 4 details the films produced under different atmospheric conditions (Figure 1 C). Each group contains eight thin films measured at five distinct positions to ensure spatial homogeneity. The uniformity of the UV-Vis spectra across these samples is notable, suggesting a consistent film thickness and composition regardless of the atmospheric conditions during fabrication. The standard deviation ( $s$ ) and coefficient of variation ( $CV$ ) values at 770 nm and 850 nm, as shown in panel F, offer quantitative insight into the uniformity of the films at key wavelengths, which are particularly interesting for their role in their absorption properties.

The analysis of Figure 4 underscores the importance of consistent absorption across the films. The negligible differences observed in absorption under various conditions point to a reliable thickness and quality of the initial thin films. This consistency is a positive indicator; however, it also suggests the absence of distinct quality control features within the UV-Vis spectra alone. In short conclusion, the UV-Vis absorption spectra serve as reliable optical markers for assessing the uniformity and thickness of the PSK PV layers, which are essential for their function. Nevertheless, to fully understand the quality of perovskite films, we must consider additional markers.





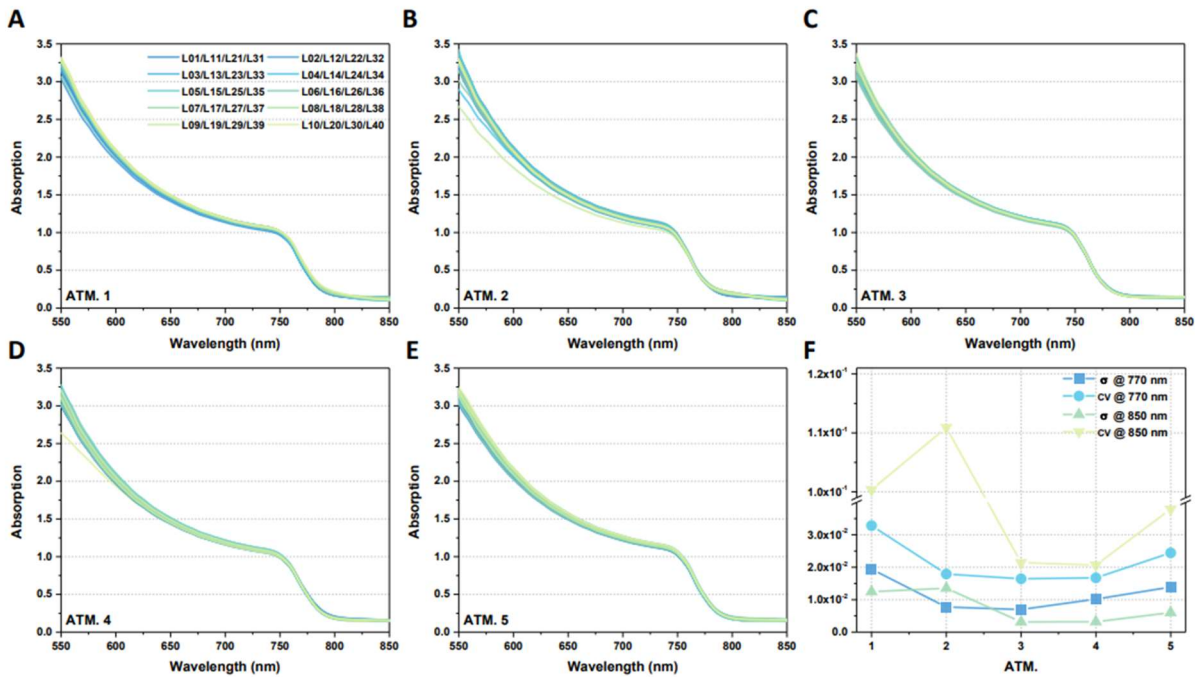


Figure 4: Comparative UV-Vis absorption spectra and variability analysis of PSK films. Panels A-E display the absorption spectra for eight thin film samples fabricated under five distinct atmospheric conditions (Figure 1C, ATM. 1-5), with each film measured at five separate points to assess intra-sample uniformity. Panel F illustrates the statistical analysis of the films' absorption at 770 nm and 850 nm, quantified by standard deviation ( $\sigma$ ) and CV, across different atmospheres, providing insight into inter-sample consistency and potential optical markers for film quality assessment [9].

Following the evaluation of uniformity and thickness through UV-Vis absorption, we extend our analysis to the dynamic optical behavior of the films using TRPL spectroscopy. This technique allows us to probe deeper into the electronic properties and quality of the perovskite films produced, which is essential in carefully selecting optical markers for fabrication.

Figure 5 presents the TRPL decay spectra of metal-halide perovskite films fabricated under different parameters in optimization step 5 (Figure 1 C bottom). The spectra indicate multi-exponential decay profiles characteristic of perovskite materials, revealing the complex nature of carrier recombination in these films. Notably, the decay curves across various dispensing timings of chlorobenzene solvent are closely aligned, signifying that these timing variations do not significantly alter the electronic properties of the films.

The consistent overlap of decay profiles across the sets underscores a reproducible fabrication process. Moreover, the similar lifetimes extracted from these profiles suggest that the carrier dynamics, critical to device performance, remain stable regardless of the minor variations in solvent dispensing timing. However, the intensity variations observed within the initial decay phase may indicate differences in quantum efficiency or surface recombination velocities among the films. However, these are not conclusively determined by TRPL alone.

The TRPL data, while affirming the homogeneity and reproducibility of electronic properties, do not provide distinct features that could serve as direct markers for controlling the timing for quenching



of Perovskite PV layers. Although the TRPL results are consistent with the absorption data in confirming reproducibility, the lack of discernable quality control markers within the TRPL decay curves suggests that TRPL alone may not suffice for comprehensive quality assessment.

As an outcome, the TRPL insights, alongside the UV-Vis absorption analysis, confirm the reproducibility of our film fabrication process. However, the absence of explicit quality control features within the TRPL decay data implies that while TRPL is an effective tool for verifying consistency, it must be supplemented with additional techniques or metrics to establish a complete quality control framework for the perovskite PV layers.

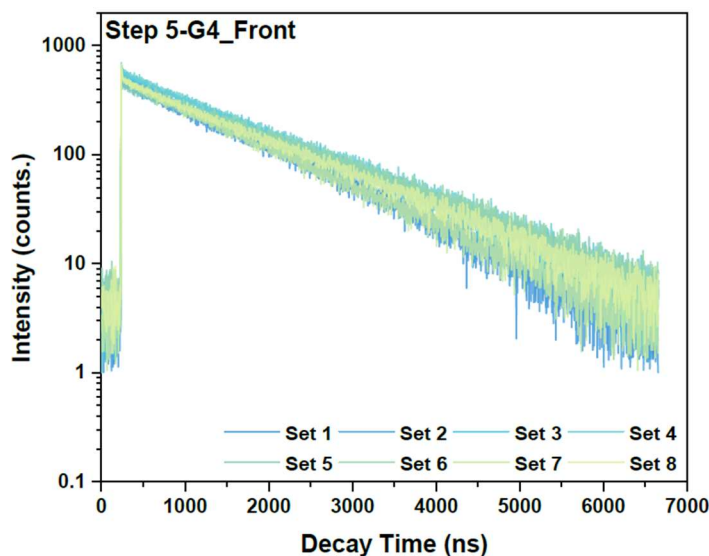


Figure 5: TRPL decay spectra for consistency analysis in PSK film fabrication. TRPL decay spectra of metal-halide perovskite films, highlighting the reproducibility of electronic properties across films fabricated with varying 120  $\mu\text{l}$  chlorobenzene dispensing timings (3 to 19 seconds) during step 5 (Figure 1 C bottom). The closely matching decay profiles across different parameters indicate a stable carrier recombination dynamic without discernible quality control markers for the manufacturing process [9].

Transitioning from the time-resolved photoluminescence analysis, which highlighted consistent electronic properties but lacked explicit quality control markers, we now focus on steady-state photoluminescence spectroscopy. This technique allows us to probe the optoelectronic quality of the films more directly and refine our selection of optical markers.

Figure 6 provides a statistical distribution of PL peak positions, widths, and integrals for films fabricated under five distinct atmospheric conditions (Figure 1 C top). The data presented in panels A through C give us a quantitative assessment of the photoluminescent behavior of the films, a direct consequence of their electronic structures and a sensitive indicator of their quality.

Analysis of panel A of PL peak positions reveals a range of bandgap energies, with narrower distributions for ATM. 4 and 5 suggesting a higher consistency in electronic properties. The PL peak width distribution in Panel B indicates the variation in material purity and defect states, with ATM. 4



and 5 again showing a tighter grouping, hinting at improved film quality. The distribution in panel C of PL peak integrals, reflecting the relative photoluminescence yield, suggests that films from ATM 4 and 5 exhibit a higher optical quality and fewer non-radiative recombination pathways. It becomes apparent that while there is significant variability in PL parameters for ATM. 1 to 3, the reduced spread in ATM. 4 and 5 indicates a more uniform production outcome. The PL spectroscopy data, represented in Figure 6, underscores the value of PL as a primary optical metric for assessing film quality and uniformity during the perovskite solar cell fabrication.

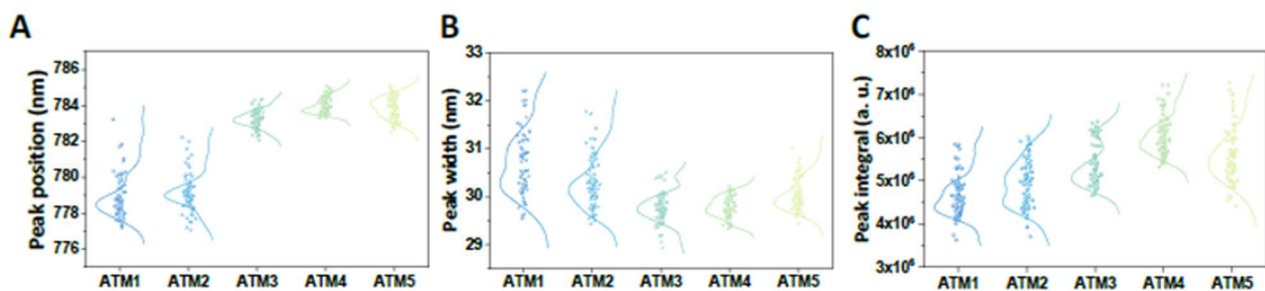


Figure 6: PL parameter variability across atmospheric conditions in PSK film fabrication. Panels A-C depict the statistical distributions for photoluminescence peak position, peak width, and peak integral for perovskite films fabricated under five different atmospheric conditions (ATM. 1-5). These plots highlight the sensitivity of PL characteristics as optical markers for assessing film quality, uniformity, and the consistency of the fabrication process [9].

## 4. THE ROLE OF PL MARKERS IN CONTROLLING THE TIMING FOR QUENCHING

Advancing from the consistent findings of film quality and uniformity inferred from the steady-state PL optical marker, our focus now shifts to the integral role of PL markers in fine-tuning the quenching process. The significance of the PL peak positions, as depicted in Figure 7, lies in their direct correlation to the optimal timing of the quenching step during the film's fabrication. The data, which details the distribution of PL peak positions for the front side of the films across several parameter variations steps (Figure 1C bottom), underscores the influence of rotation speed for antisolvent dropping and antisolvent volume and dispense time delay conditions and other processing parameters on the crystalline of the films and their optoelectronic properties.

Through the sequential optimization process, we analyzed the PL peak positions in relation to the tip heights, and antisolvent dispensing speeds, and antisolvent dispensation delay, among other variables. This analysis revealed that a consistent PL peak position across different steps indicates a robust and stable film manufacturing process, essential for achieving the desired optoelectronic properties of the perovskite PV layers.



Moreover, the narrow distribution of PL peak positions, particularly in Step 5 involving antisolvent volume and delay timing, serves as a critical optical marker. It signifies that the films have undergone sufficient crystallization, making it an opportune moment for quenching to preserve the material's intrinsic properties. The spatial consistency of PL emission, peak broadening, and intensity across the manufacturing process validate the use of these markers for precise timing control in quenching. These PL characteristics might emerge as reliable indicators of the homogeneity and quality of the halide perovskites.

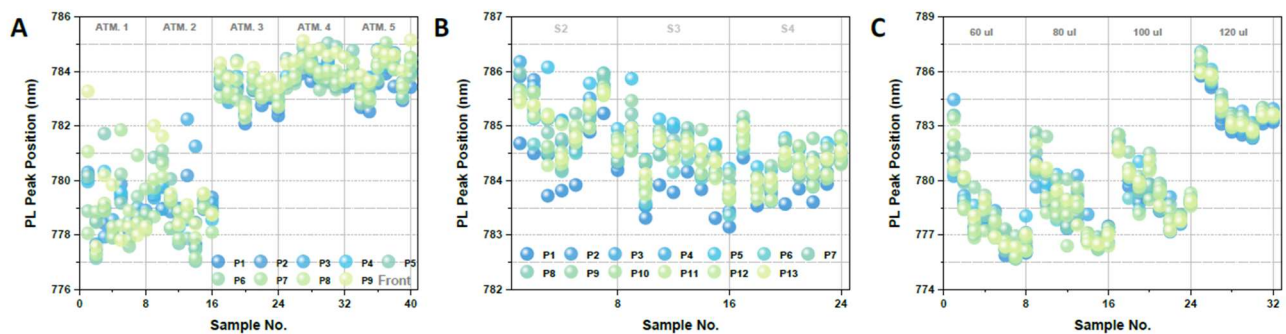


Figure 7: Variations in PL peak position across film fabrication variation Steps. Panels A-C exhibit the statistical distribution of photoluminescence peak positions for perovskite films at various stages of production variations, corresponding to different variations in fabrication steps from atmosphere control to antisolvent dynamics (Step 1, Steps 2-4, and Step 5, Figure 1C bottom). These distributions provide insights into the effect of manufacturing variables on the PL properties of the films [9].

Moving from evaluating PL peak positions, which established a stable optical marker, we now advance to a detailed examination of additional steady-state photoluminescence properties. Figure 8 offers a detailed statistical analysis of the full width at half maximum (FWHM) and integrated photoluminescence intensity, reflecting the microstructure of the films and radiative recombination efficiency under various processing conditions. Panels A-C present the FWHM variability, with consistent readings suggesting the presence or absence of uniform crystallinity structure within films and potential deviation in defect concentration. Panels D-F depict the integrated PL intensity, with a tighter distribution indicating a more consistent semiconductor quality. Variability in this parameter can reflect differences in semiconductor quality and highlight the presence of non-radiative recombination pathways. Incorporating FWHM and integrated intensity with PL analysis could act as a sensitive measure for assessing film quality and uniformity. The statistical distribution of these metrics across different processing variation steps underscores the potential application of those optical markers, with particular attention to the quenching phase (Figure 8 B, C, E, F). The FWHM PL and integrated PL intensity optical markers can indicate the homogeneity and quality of fabricated films. By consistently achieving narrow distributions for these markers, we can confirm a controlled deposition process and effectively guide the timing of quenching to lock in the desirable material properties.



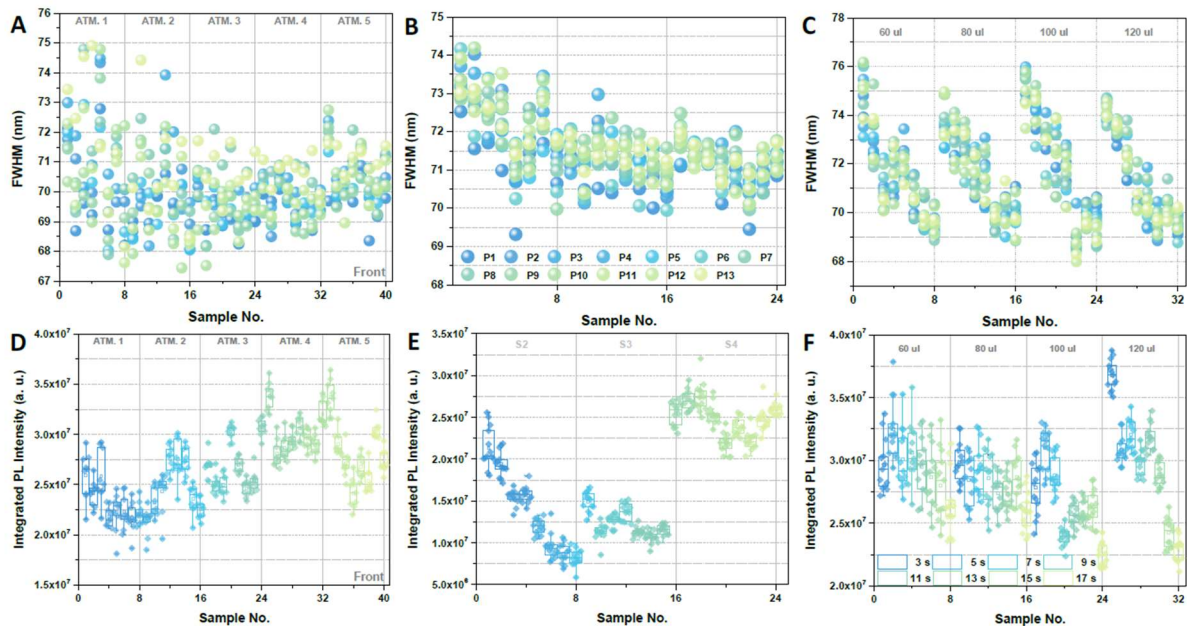


Figure 8: PL Emission characteristics and quality metrics of perovskite films across fabrication variation Steps. (A-C) Display the statistical distribution of the FWHM from PL spectra, indicating the emission linewidth consistency. (D-F) Provide a grouped box plot representation of the integrated photoluminescence intensity, reflecting the radiative recombination efficiency. These metrics are shown for films processed under varied conditions in Step 1 (atmosphere), Steps 2 to 4 (tip height, antisolvent dispense speed, rotation speed), and Step 5 (antisolvent volume and dispense timing delay), elucidating the impact of each step on film quality and uniformity [9].

Building upon our established understanding of PL spectroscopy as an indicator of film consistency, we now turn to the analysis of spatial PL intensity distribution, a crucial aspect for evaluating PV device performance. This step is essential, considering that the collective performance of the entire active layer beneath the contacts determines PV efficiency.

Figure 9 provides contour maps that display the distribution of PL intensity across the surfaces of perovskite thin films, with each map corresponding to films treated with different CB antisolvent feeding timings. These quenching timings show a prominent impact on the crystallization process of the films, directly influencing their quality and uniformity.

The contour maps in Figure 9 reveal variations in PL intensity across the films, indicating differences in crystallization and film thickness dependently on the timing parameter for antisolvent quenching. Uniformity in these maps is essential as it reflects a consistent crystallization process across the film surface and thickness, which is crucial for achieving uniform PV device performance. The variations in PL intensity, shown through the color gradations in the maps, indicate the inhomogeneity over the film area and the quenching process effectiveness. Furthermore, analyzing these PL intensity distributions aids in fine-tuning the fabrication process, particularly the critical step of antisolvent quenching timing. By assessing the uniformity of the PL response, we can optimize this timing to ensure that the films exhibit the desired crystallization and material properties throughout the pixel area. The contour maps of PL intensity distribution act as sensitive optical markers for assessing the



homogeneity and quality of perovskite layer crystallization. This analysis is integral for guiding the precise timing of quenching in the fabrication process. As revealed in these maps, the consistency of PL intensity across the film area indicates the potential pixel device performance, thereby linking the microscopic film properties to the potential macroscopic device efficiency. Through this PL analysis, we can confirm the controlled deposition process and effectively determine the optimal timing for quenching, leading to high-quality perovskite PV layers with reproducible and reliable performance.

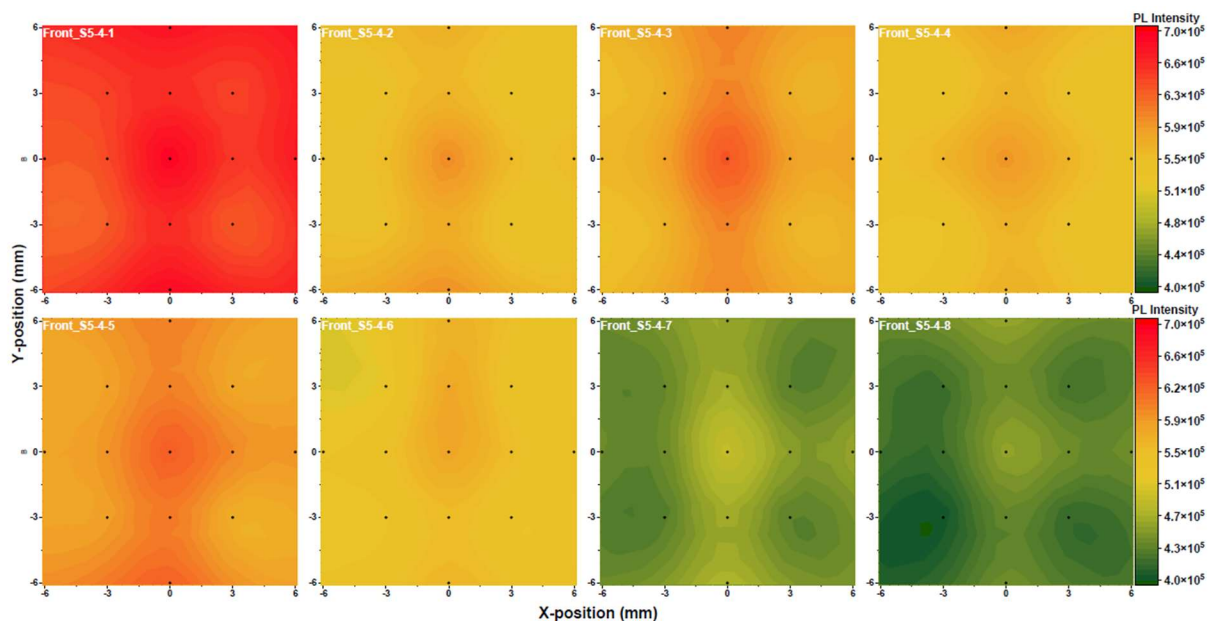


Figure 9: Spatial distribution of PL intensity in perovskite films with variable antisolvent quenching timings. This contour map array showcases the PL intensity distribution measured at 13 evenly distributed spatial points (P1-P13) across the surface of perovskite thin films fabricated with different CB antisolvent feeding times (3, 5, 7, 9, 11, 13, 15, 17 seconds). The maps indicate film uniformity and crystallization homogeneity, which is critical for evaluating potential photovoltaic device performance reproducibility across varied film processing conditions [9].

## 5. CASE STUDY: PEROVSKITE SOLAR CELL FABRICATION

Moving from our in-depth PL analysis, we apply these insights to fabricating perovskite solar cells. This section will evaluate the practical application of our PL findings in the context of solar cell performance. We explore how the uniformity in PL intensity and other PL parameters across the perovskite layer, a direct result of controlled quenching, contributes to the overall efficiency and consistency of the solar cells. The architecture of the PV device is depicted in Figure 10, providing a schematic representation of a metal halide perovskite solar cell, highlighting the layered structure. The stack consists of a glass substrate covered with an ITO layer (ITO Glass), an electron transport layer ( $\text{SnO}_2$ ), an active perovskite layer, a hole transport layer (PDCBT), and the top electrode (Au).



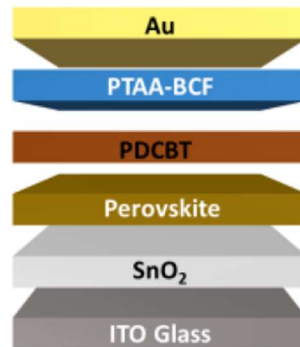


Figure 10: Structure schematic of a metal halide perovskite solar cell assembled using the SPINBOT platform in ambient air [9].

In assessing the impact of our PL findings on solar cell efficiency, Figure 11 presents the IV characteristics of perovskite solar cells fabricated under various quenching timings parameters. The IV curves are shown for four different sets of cells, each set corresponding to a specific CB dispense timing: 3 seconds (A), 5 seconds (B), 7 seconds (C), and 9 seconds (D).

The analysis of these IV curves reveals several aspects:

**Photocurrent Density:** The  $J_{sc}$  values across A and B panels are relatively consistent, suggesting that the light absorption capability of the cells is mainly unaffected by the variations in quenching timing. However, panels C and D show significant deviations, which correlate with conclusions from previous sections illustrated in Figures 8 and 9.

**Open-Circuit Voltage:** The variations in  $V_{oc}$  might be linked to the changes in perovskite film quality due to different quenching timings. A higher  $V_{oc}$  generally indicates better charge separation and lower recombination rates linked to the film and crystallinity quality.

**Fill Factor:** The FF variations across the panels provide insights into the quality of the cells, including the extent of recombination and resistance within the cells.

**Power Conversion Efficiency:** The range of PCE values demonstrates the overall impact of antisolvent quenching timing on device performance.

The correlation between the PL analysis and the IV performance looks evident, considering findings from section 4. Consistent FWHM and integrated PL intensity, indicative of uniform crystallinity, are reflected in the IV characteristics, particularly in PCE. The contour maps from Figure 9, showing PL intensity distribution, further reinforce the importance of homogenous crystallization for achieving uniform device performance. The IV analysis for each group of devices highlights the impact of proper tuning process parameters, informed by section 4 of optical markers, on the optimized performance of the devices.

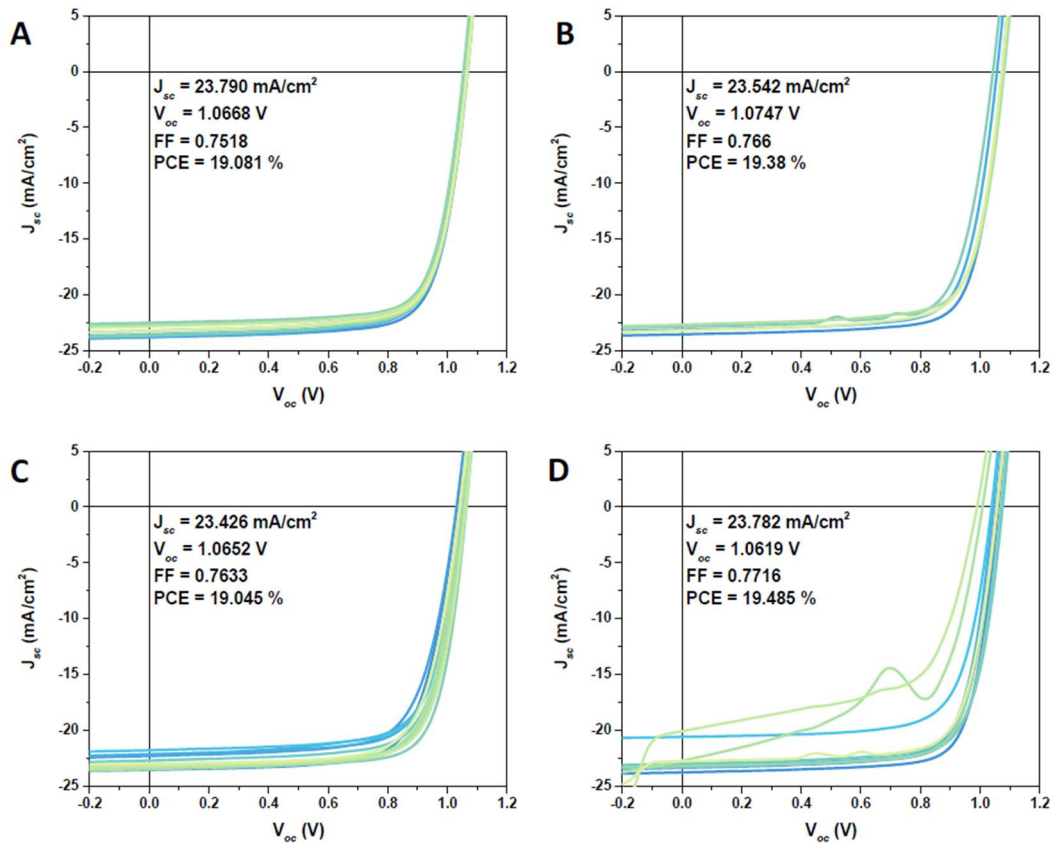


Figure 11: IV Characterization of perovskite solar cells with varied antisolvent quenching timings. The figure highlights the impact of different chlorobenzene antisolvent quenching timings (3, 5, 7, and 9 seconds) on the device performance metrics,  $J_{sc}$ ,  $V_{oc}$ , FF, and PCE [9].

Furthermore, perovskite solar cell performance, as illuminated by Figure 12, draws a direct line between the detailed photoluminescence findings and the electrical characteristics of the solar cells. In Panel A, while displaying a general similarity in electrical performance, the IV curves across different CB dispense timings deviate to reflect the influence of the dispense timing on device quality and efficiency. The spread in  $V_{oc}$  and FF values from Panel B indicates how the antisolvent dispense timing modulates the electric field across the device. This modulation is inherently linked to the crystallization process tracked by our PL analysis. The variations in  $J_{sc}$  and PCE depicted in Panel C, aligning with our observations from the previous section about the optoelectronic properties of films, underscore the influence of the quenching process on charge generation and recombination within the device.

The variations observed in the IV curves, as indicated in Figure 12, may reflect differences in the crystalline structure and defect levels within the perovskite films. These differences could be related to broader FWHM or lower integrated PL intensity, as previously analyzed in Figure 8. Additionally, the uniformity in PL intensity distribution across the film surface, demonstrated in the contour maps of Figure 9, appears to correspond with the consistent performance of the devices in the IV analysis.





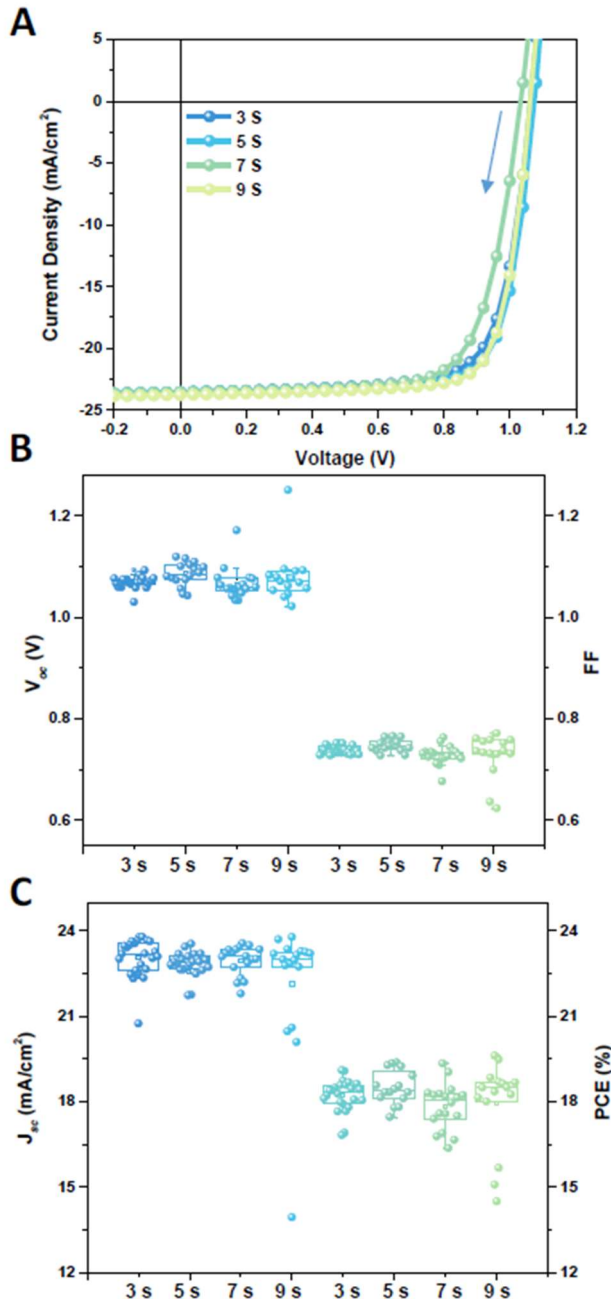


Figure 12: Performance characterization of perovskite solar cells with variations in antisolvent dispensing timing during fabrication. Panel A shows the IV curves under reverse bias, illustrating the electrical response of the champion devices for each group. Panels B and C present the distribution of  $V_{oc}$ , FF, and the combined  $J_{sc}$  with PCE, respectively, highlighting the impact of CB antisolvent dispense timing (3, 5, 7, and 9 seconds) on device performance [9].

## 6. CONCLUSION

In order to identify optical markers for controlling quenching timing in perovskite PV layers, we employed a multi-faceted approach using UV-Vis absorption, PL, and TRPL. Our analysis, grounded



in the combination of the SPINBOT automated platform with high throughput characterizations revealed the following key findings:

**UV-Vis Absorption Spectroscopy:** As Figure 4 illustrates, we observed uniform UV-Vis absorption spectra across various samples, suggesting consistent film thickness and composition. However, these spectra lacked distinct quality control features, indicating the need for additional markers to fully assess film quality.

**Time-Resolved Photoluminescence:** TRPL analysis in Figure 5 showed stable electronic properties across different fabrication parameters, but it did not provide clear quality control markers. This highlighted the necessity of integrating additional techniques for a comprehensive quality assessment.

**Steady-State Photoluminescence Spectroscopy:** In Figure 6, we analyzed PL peak positions, widths, and integrals, finding variability in these parameters under different conditions. This analysis established PL spectroscopy as a good optical metric for assessing film quality and uniformity.

**PL FWHM and Integrated Intensity:** statistical analysis of FWHM and integrated PL intensity in Figure 8 provided insights into film microstructure and radiative recombination efficiency. These markers were instrumental in guiding the timing of quenching during film fabrication.

**Spatial PL Intensity Distribution:** The contour maps in Figure 9 revealed variations in crystallization and film thickness based on antisolvent quenching timing, emphasizing the importance of PL intensity distribution as an indicator of film homogeneity.

**Perovskite Solar Cell Fabrication:** Applying these insights to solar cell fabrication, we assessed device performance through IV characteristics in Figure 11. This analysis demonstrated the impact of different quenching timings on key performance metrics like photocurrent density, open-circuit voltage, fill factor, and power conversion efficiency.

**IV Curve Correlation with PL Analysis:** Figure 12 connected our PL findings with the electrical characteristics of solar cells. Variations in IV curves reflected differences in crystalline structure and defect levels, validating the role of PL markers in optimizing device performance.

In summary, our study established the role of selecting appropriate optical markers for controlling quenching timing in perovskite PV layers. This selection is pivotal in ensuring uniform film quality and optimizing the performance of perovskite solar cells, thereby contributing to advancements in photovoltaic technology.



## 7. REFERENCES

- [1] Gratia, Paul, et al. "The many faces of mixed ion perovskites: unravelling and understanding the crystallization process." *ACS Energy Letters* 2.12 (2017): 2686-2693.
- [2] Qin, Minchao, Pok Fung Chan, and Xinhui Lu. "A systematic review of metal halide perovskite crystallization and film formation mechanism unveiled by in situ GIWAXS." *Advanced Materials* 33.51 (2021): 2105290.
- [3] Merdasa, Aboma, et al. "Eye in the process: Formation of "triple cation" perovskite thin films rationalized by in-situ optical monitoring." (2020).
- [4] Rehmann, Carolin, et al. "Origin of Ionic Inhomogeneity in  $\text{MAPb}(\text{I}_x\text{Br}_{1-x})_3$  Perovskite Thin Films Revealed by In-Situ Spectroscopy during Spin Coating and Annealing." *ACS Applied Materials & Interfaces* 12.27 (2020): 30343-30352.
- [5] Camus, Christian, et al. "Going beyond Alchemy: In-situ Analysis of Perovskite Growth by Optical Reflectance." *2020 47th IEEE Photovoltaic Specialists Conference (PVSC)*. IEEE, 2020.
- [6] Rehmann, C., et al. "Role of solution concentration in formation kinetics of bromide perovskite thin films during spin-coating monitored by optical in situ metrology." *RSC advances* 12.50 (2022): 32765-32774.
- [7] Fong, Patrick Wai-Keung, et al. "Printing high-efficiency perovskite solar cells in high-humidity ambient environment—an in situ guided investigation." *Advanced Science* 8.6 (2021): 2003359.
- [8] Schackmar, Fabian, et al. "In Situ Process Monitoring and Multichannel Imaging for Vacuum-Assisted Growth Control of Inkjet-Printed and Blade-Coated Perovskite Thin-Films." *Advanced Materials Technologies* 8.5 (2023): 2201331.
- [9] Zhang, Jiyun, et al. "Optimizing Perovskite Thin-Film Parameter Spaces with Machine Learning-Guided Robotic Platform for High-Performance Perovskite Solar Cells." *Advanced Energy Materials* (2023): 2302594.

